MBoC | ARTICLE

TFIIIC localizes budding yeast *ETC* sites to the nuclear periphery

Shin-ichiro Hiraga[a,*], Sotirios Botsios[a,*], David Donze[b], and Anne D. Donaldson[a]
[a]Institute of Medical Sciences, University of Aberdeen, Aberdeen AB25 2ZD, Scotland, United Kingdom; [b]Department of Biological Sciences, Louisiana State University, Baton Rouge, LA 70803

ABSTRACT **Chromatin function requires specific three-dimensional architectures of chromosomes. We investigated whether *Saccharomyces cerevisiae* extra TFIIIC (*ETC*) sites, which bind the TFIIIC transcription factor but do not recruit RNA polymerase III, show specific intranuclear positioning. We show that six of the eight known *S. cerevisiae ETC* sites localize predominantly at the nuclear periphery, and that *ETC* sites retain their tethering function when moved to a new chromosomal location. Several lines of evidence indicate that TFIIIC is central to the *ETC* peripheral localization mechanism. Mutating or deleting the TFIIIC-binding consensus ablated *ETC* -site peripheral positioning, and inducing degradation of the TFIIIC subunit Tfc3 led to rapid release of an *ETC* site from the nuclear periphery. We find, moreover, that anchoring one TFIIIC subunit at an ectopic chromosomal site causes recruitment of others and drives peripheral tethering. Localization of *ETC* sites at the nuclear periphery also requires Mps3, a Sad1-UNC-84–domain protein that spans the inner nuclear membrane. Surprisingly, we find that the chromatin barrier and insulator functions of an *ETC* site do not depend on correct peripheral localization. In summary, TFIIIC and Mps3 together direct the intranuclear positioning of a new class of *S. cerevisiae* genomic loci positioned at the nuclear periphery.**

Monitoring Editor
Orna Cohen-Fix
National Institutes of Health

Received: Apr 26, 2011
Revised: Feb 23, 2012
Accepted: Apr 4, 2012

INTRODUCTION

The three-dimensional organization of the genetic material in nuclear space is integrally related to chromatin function (reviewed by Sexton *et al.*, 2007). In some higher eukaryotic cells, for example, chromosomes occupy specific nuclear "territories" that reflect their gene density and heterochromatin content (Croft *et al.*, 1999; Tanabe *et al.*, 2002). Typically, chromosome regions containing a high proportion of nontranscribed sequence display localization to the nuclear periphery (reviewed in Towbin *et al.*, 2009). Silenced chromatin in yeast cells is preferentially positioned to the nuclear periphery (Maillet *et al.*, 2001), and artificial tethering to the nuclear rim partially restores transcriptional repression by a compromised silencer (Andrulis *et al.*, 1998). Gene expression in metazoans can also be modified by manipulating its intranuclear positioning (Finlan *et al.*, 2008). The spatial arrangement of metazoan chromosomes appears to be tissue specific (Parada *et al.*, 2004) and becomes reorganized during differentiation (Kim *et al.*, 2004).

Studies of chromosome spatial organization have revealed specific intranuclear positioning of particular chromosome domains. Localization of telomeres at the nuclear periphery has been described in the budding yeast *Saccharomyces cerevisiae* (Gotta *et al.*, 1996), in fission yeast *Schizosaccharomyces pombe* (Funabiki *et al.*, 1993), in human cells (de Lange, 1992; Croft *et al.*, 1999), and in other organisms (Chung *et al.*, 1990; Dawe *et al.*, 1994). The 64 telomeres of diploid budding yeast cells cluster at the nuclear periphery in three to eight discrete foci (Klein *et al.*, 1992; Gotta *et al.*, 1996), with the subtelomeric sequences being subject to transcription silencing (Gottschling *et al.*, 1990). Other genomic regions also exhibit specific spatial organization in the nucleus that is related to biological function. For example, the ribosomal DNA is localized to the nucleolus (Hartung *et al.*, 1979; Dujon, 1998; Kalmarova *et al.*, 2007), whereas during interphase yeast centromeres cluster near

This article was published online ahead of print in MBoC in Press (http://www.molbiolcell.org/cgi/doi/10.1091/mbc.E11-04-0365) on April 11, 2012.

*These authors contributed equally.

Address correspondence to: Anne D. Donaldson (a.d.donaldson@abdn.ac.uk).

Abbreviations used: ChIP, chromatin immunoprecipitation; COC, chromosome-organizing-clamp; ETC, extra TFIIIC; GFP, green fluorescent protein; Pol III, RNA polymerase III; SUN, Sad1-UNC-84; TFIIIB, transcription factor IIIB; TFIIIC, transcription factor IIIC.

the spindle pole body, opposite the nucleolus (Guacci *et al.*, 1997; Jin *et al.*, 1998). In addition, it has been reported that active *S. cerevisiae* tRNA genes tend to be localized to the nucleolus (Bertrand *et al.*, 1998; Thompson *et al.*, 2003), which is important for tRNA gene-mediated silencing (Kendall *et al.*, 2000). Additional examples of directed chromosome positioning include the relocalization to the nuclear periphery of specific genes upon transcriptional activation (e.g., *GAL* genes, *INO1* locus; Brickner and Walter, 2004; Casolari *et al.*, 2005; Schmid *et al.*, 2006). The fact that peripheral localization has been implicated in transcription activation as well as repression led to models proposing that the nuclear envelope comprises a mosaic of zones favoring either transcriptional induction or silencing.

The *S. pombe* RNA polymerase III transcriptional apparatus is implicated in chromosome spatial organization. Eukaryotic RNA polymerase III (Pol III) is responsible for the transcription of small structural RNAs, including tRNAs, 5S rRNA, and other small nuclear and cytoplasmic RNAs (reviewed by Dieci *et al.*, 2007). The Pol III transcription machinery is highly conserved and consists of the multisubunit Pol III polymerase and two transcription factor complexes (TFIIIB and TFIIIC; Kassavetis *et al.*, 1990). An additional factor (TFIIIA) is required only for *5S rDNA* transcription. Pol III–transcribed genes share specific sequence and structural properties, including conserved *A* and *B box* sequences typically found within the coding region (Galli *et al.*, 1981). These internal control regions are recognized by the six-subunit complex TFIIIC (Baker *et al.*, 1986; Bartholomew *et al.*, 1990). The *B box* sequence is conserved in all eukaryotes (GGTTCGANTCC), and mutation of the internal cytosine inactivates both TFIIIC binding and Pol III transcription of a tRNA gene (Newman *et al.*, 1983; Baker *et al.*, 1986; Marzouki *et al.*, 1986). Once assembled, TFIIIC recruits TFIIIB to an ~50–base pair, AT-rich region upstream of the transcription start site. After recruitment by TFIIIC, TFIIIB in turn recruits Pol III for transcription initiation (Kassavetis *et al.*, 1990, 1997).

Chromatin boundary elements function to separate chromatin domains, either by insulating promoters from transcriptional activation or by acting as barriers to the propagation of repressive heterochromatin (West *et al.*, 2002). A study in the fission yeast *S. pombe* revealed a role for the RNA polymerase III apparatus, and TFIIIC in particular, in boundary function and genome organization. Chromatin boundary elements called "inverted repeats" (*IR*s) contain multiple *B box* sequences but are not transcribed. *IR* elements were shown to bind TFIIIC but not other Pol III factors or Pol III itself, suggesting that TFIIIC binding may mediate chromatin boundary function (Noma *et al.*, 2006). These TFIIIC-bound *IR* insulators were found to be predominantly associated with the nuclear periphery. It was suggested that such loci act as so-called chromosome-organizing-clamp (*COC*) sites that tether chromosomal regions to the nuclear periphery, possibly mediating three-dimensional organization of the fission yeast genome (Noma *et al.*, 2006). However, the mechanism of peripheral localization is unclear.

In a genome-wide survey of Pol III apparatus occupancy in *S. cerevisiae*, eight intergenic loci were identified that display TFIIIC occupancy but no significant recruitment of other Pol III factors (Moqtaderi and Struhl, 2004). These loci were called extra TFIIIC (*ETC*) sites. Of interest, these loci tend to lie in divergent intergenes. All eight loci share a sequence that resembles a *B box* consensus, but with an additionally conserved 10-base extension to the 3′ side (Moqtaderi and Struhl, 2004). The *ETC* extended *B box* consensus sequences are highly conserved among sensu stricto yeast species, suggesting an important biological function. Two additional *S. cerevisiae* genome-wide studies of Pol III–binding sites (Harismendy *et al.*, 2003; Roberts *et al.*, 2003) identified several of the same *ETC* loci, as well as other sites that recruit partial Pol III complexes. Recently *ETC* loci were shown to be able to function as chromatin insulators, blocking gene activation if artificially inserted between an upstream activation sequence (UAS) and its transcriptional start site (Simms *et al.*, 2008; Valenzuela *et al.*, 2009). In addition, *ETC6* was shown to have an insulator-like function in its natural context. Two *ETC* sites (*ETC2* and *ETC4*) can also function in reporter constructs as barriers to the spread of heterochromatin, suggesting a role for TFIIIC in regulating Pol II–transcribed genes (Simms *et al.*, 2008; Valenzuela *et al.*, 2009; Kleinschmidt *et al.*, 2011). Although several studies suggested that TFIIIC binding in the absence of TFIIIB is sufficient for such insulator and barrier activities, a recent investigation found TFIIIC-mediated insulation was increased in the presence of bound TFIIIB and was compromised in various histone modifier and remodeler mutants (Valenzuela *et al.*, 2009).

In a recent interesting development, Moqtaderi *et al.* (2010) identified >1865 *ETC* loci in the human genome that recruit TFIIIC but not other Pol III apparatus components. Human *ETC* (*hETC*) loci are preferentially located between closely spaced, divergently transcribed Pol II genes, reminiscent of *S. cerevisiae ETC*s. *hETC* loci are characterized by one of two sequence motifs: either a *B box* sequence or a novel motif loosely related to the binding motif for the ET transcription factor family (Moqtaderi *et al.*, 2010). Thousands of *ETC* sites have also been identified in the mouse genome (Carriere *et al.*, 2012).

We investigated whether *S. cerevisiae ETC* sites mediate positioning to the nuclear periphery. By fluorescently tagging all eight known *ETC* sites, we showed that the majority of *ETC* loci localize predominantly to the nuclear periphery. The *ETC B box* consensus is necessary for peripheral positioning, and an *ETC* locus is sufficient to cause peripheral localization if transferred to another chromosomal region. We find that the TFIIIC complex itself directs peripheral tethering through a pathway that involves the inner nuclear membrane protein Mps3. Surprisingly, however, it appears that peripheral localization of an *ETC* site is not required for its insulator or barrier activity.

RESULTS

ETC loci act as *COC*s in *S. cerevisiae*

We investigated whether *ETC* loci in *S. cerevisiae* are tethered to the nuclear periphery. *ETC* sites can be microscopically visualized in live cells using the chromosome dot system. An *ETC* site is tagged by inserting an array of *lac* operator repeats (Figure 1A) in cells expressing the Lac repressor protein fused to green fluorescent protein (GFP; LacI-GFP; Robinett *et al.*, 1996). Recruitment of LacI-GFP to the tagged *ETC* locus allows its visualization as a bright dot (Figure 1B). To facilitate measurement of the position and movement of the *ETC* dot, the nuclear envelope is also marked using a GFP-fused allele of the nuclear pore component *NUP49* (Belgareh and Doye, 1997). Quantification of the chromosomal *ETC* dot position is performed using the "three-zoning" method (Taddei and Gasser, 2004), in which the dot is scored to one of three concentric zones of equal surface area (Figure 1C). A randomly positioned locus shows equal distribution among the three zones (~33% in zones 1–3), whereas a locus positioned at the nuclear periphery is preferentially observed in zone 1 (Figure 1, C and D). Cell cycle position is assessed according to bud size (see *Materials and Methods*).

ETC2 lies on the left arm of chromosome XV (genome coordinate: XV, 58539–58758), more than 59 kb from telomere XV-L (Figure 1A; Moqtaderi and Struhl, 2004). The intergene neighboring *ETC2* was GFP tagged as described. We found that in the majority of interphase cells, the *ETC2* locus resides in zone 1

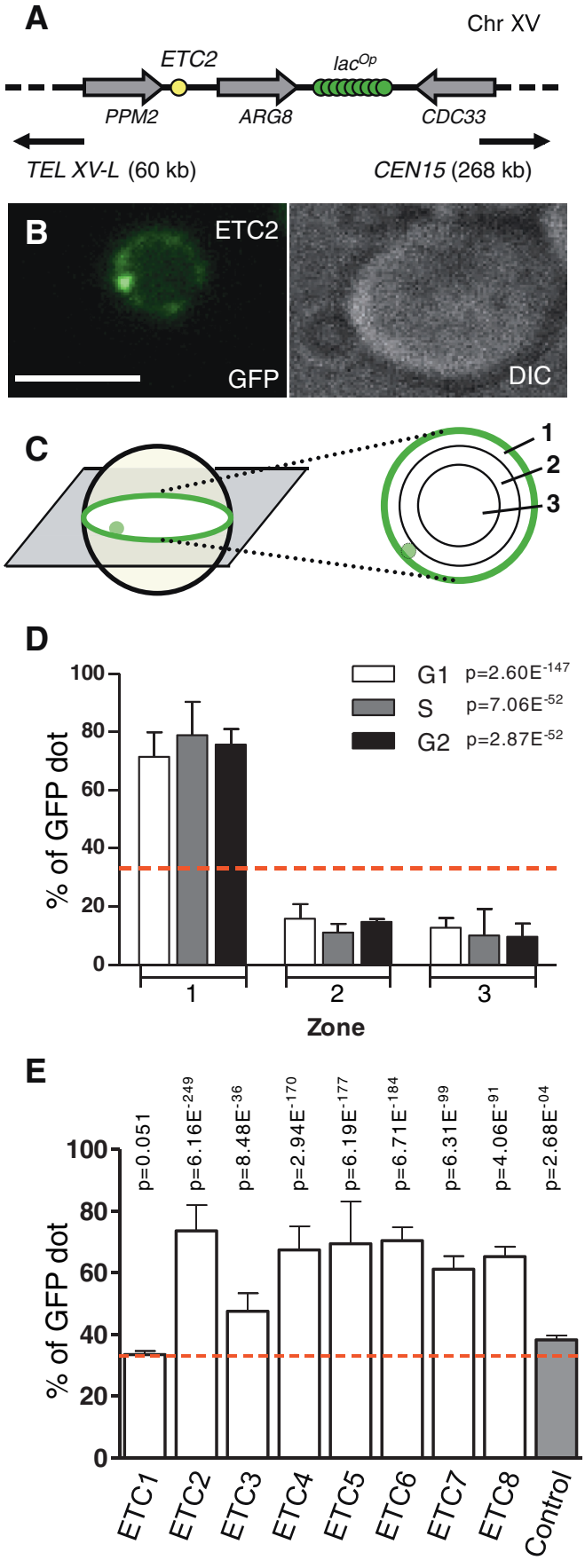

FIGURE 1: Chromosome dot assay reveals peripheral localization of *ETC* sites. (A) Illustration of strain construct used to test intranuclear positioning of *ETC2*, located within *PPM2-ARG8* intergene on chromosome XV. The neighboring intergene (*ARG8-CDC33*) was GFP tagged by *lac*^{Op} array insertion. The center of the *lac*^{Op} array is 6.6 kb from the *ETC2* locus. Chromosome dot strains to visualize other *ETC* sites were constructed similarly (see Table 1 in *Materials and Methods*). (B) Typical images of strains with chromosomal *ETC2* tag, seen as a bright dot. The strain also expresses Nup49-GFP to visualize the nuclear membrane, seen as a dimmer ring. Right, DIC image . Scale bar, 3 μm. (C) Evaluation of *ETC*-site localization. Localization of the GFP dot was scored against three concentric zones with equal surface area as described in *Materials and Methods*. (D) *ETC2* localization, assessed separately for cells in G1 phase, S phase, and G2 phase. Percentage of cells with *ETC2* dot in each zone is plotted. (E) Percentage of cells showing peripheral (i.e., zone 1) positioning of *ETC1-8* and a *ChrVI*^{int} (control) site, plotted as the cumulative total of cells in G1, S, and G2 phases. Error bars represent SD of values obtained from independent strain isolates (n = 3, except *ETC8*, for which n = 2), for each of which at least 300 cells were inspected. Red dashed line represents the expected value (33.3%) for a randomly positioned locus. The p values were calculated by χ^2 analysis in which actual distribution was compared with a hypothetical random distribution.

(localization to zone 1 in 71.5% of G1 cells, 78.9% of S cells, and 75.7% of G2 cells; Figure 1D). In most cases in which *ETC2* was observed within zone 1, the fluorescent signal from the chromosome dot and the nuclear envelope appeared juxtaposed. Of importance, *ETC2* remains predominantly localized to the nuclear periphery in G2 phase. The cell cycle regulation of *ETC2* positioning therefore differs from that of telomeres, which become randomly localized in G2 phase. A χ^2 analysis confirmed that *ETC2* positioning during all three cell cycle phases differs significantly from random (Figure 1D).

We constructed strains in which the other seven *ETC* loci were individually fluorescently tagged and examined their subnuclear localization. Figure 1E shows the percentage of GFP dots observed at the nuclear periphery (i.e., in zone 1) for each *ETC*-tagged strain, shown as a cumulative total throughout interphase (cell cycle–staged results in Supplemental Figure S1). *ETC4*, *ETC5*, *ETC6*, *ETC7*, and *ETC8* reside in zone 1 in the majority of interphase cells (Figure 1E). All of these loci retained peripheral localization throughout interphase (Supplemental Figure S1), similar to the pattern observed for *ETC2*. A control locus (*ChrVI*^{int}) displayed random positioning.

ETC1, in contrast, exhibited virtually random positioning throughout the cell cycle (33.5%; Figure 1E). *ETC3* was also positioned largely randomly, displaying only a slight tendency toward peripheral localization (47.5%; Figure 1E).

To summarize, we found that six of the eight *ETC* loci (*ETC2*, *ETC4*, *ETC5*, *ETC6*, *ETC7*,and *ETC8*) exhibited clear peripheral subnuclear localization. The *S. cerevisiae* genome therefore contains at least six peripherally positioned *ETC* chromosome loci, which we propose are equivalent to *S. pombe COC* sites.

ETC sites do not associate with the nucleolus or telomeric foci

ETC loci share certain sequence and structural properties with tRNA genes—in particular, a *B box* consensus and TFIIIC binding. Because some tRNA genes are proposed to localize to the nucleolus (Bertrand *et al.*, 1998; Thompson *et al.*, 2003), we tested whether *ETC* loci also associate with the nucleolus. The *S. cerevisiae* nucleolus occupies a crescent adjacent to the nuclear envelope, so *ETC* positioning to the nuclear periphery does not preclude nucleolar localization. *ETC7* positioning was examined in a strain bearing an mCherry-tagged version of the nucleolar marker protein Nop1

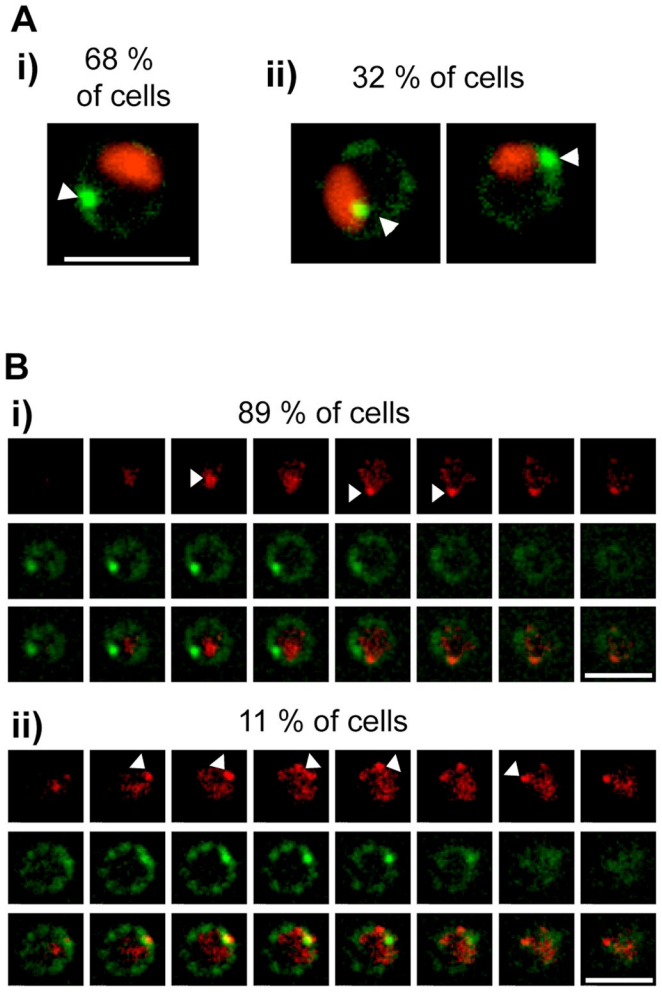

FIGURE 2: *ETC7* does not colocalize with the nucleolus and telomeres. (A) Typical images of strains carrying GFP-tagged *ETC7* and *NOP1-mCherry*, visualized as a green dot and a red crescent, respectively. Nup49-GFP reveals the nuclear rim. Sixty-eight percent of cells displayed no colocalization between *ETC7* and the nucleolus (i, left); in only 32% of cells was the *ETC7* signal immediately juxtaposed to or within the nucleolus (ii, right). White arrowheads mark the *ETC7* GFP dot. Scale bar, 3 μm. Scores represent the average from three independent strain isolates (SBY31, SBY32, and SBY33), for each of which at least 180 cells were inspected. (B) Typical Z-stack series of images showing strains carrying GFP-tagged *ETC7* and *RAP1-mCherry*. Nup49-GFP reveals the nuclear rim. Shown for Z-stack series (i) and (ii) are (top) mCherry signal (telomere foci), (middle) GFP (*ETC7* and nuclear rim), and (bottom) merged overlay. White arrowheads mark telomere foci. Scale bar, 3 μm. The majority of cells (89%) showed no coincidence of *ETC7* with telomeric foci, as series (i); in only 11% of cells was *ETC7* observed to associate with telomere clusters, as series (ii). Scores represent the average from three independent strain isolates (SBY84, SBY85, and SBY86), for each of which at least 210 cells were inspected.

(Schimmang *et al.*, 1989). Colocalization of *ETC7* with the nucleolus was scored if the chromosome dot and Nop1 fluorescent signals coincided or were juxtaposed when observed at the equatorial region in a Z-stack of images (Figure 2A). We found no tendency for *ETC7* to be located close to or within the nucleolus. The nucleolus occupies on average 30% of the nuclear volume, but *ETC7* coincided with the nucleolus in only 32.4% of interphase cells (Figure 2Aii). A χ^2 analysis confirmed this value as consistent with only random coincidence of *ETC7* with the nucleolus ($p = 0.086$). Similar results were obtained from analysis of *ETC5*, which showed 30.1% colocalization with the nucleolus (unpublished data).

S. cerevisiae telomeres form clusters at the nuclear periphery (Klein *et al.*, 1992; Gotta *et al.*, 1996). To test whether *ETC* sites colocalize with telomeres, we used a mCherry-Rap1 fusion protein to visualize the telomere foci, which appear as bright fluorescent foci at the nuclear periphery (Hayashi *et al.*, 1998; Hiraga *et al.*, 2006). In G1- and S-phase cells, these foci were predominantly localized at the nuclear envelope, as expected. Colocalization of an *ETC7* dot with a telomere focus was scored if the fluorescent signals coincided or were juxtaposed when observed in the equatorial region in a Z-stack of images (Figure 2B). We found no tendency for *ETC7* to colocalize with telomere clusters at greater-than-random incidence (11.1%; Figure 2Bii). Similar results were obtained with *ETC2* (12.9% colocalization; unpublished data).

To summarize, *S. cerevisiae ETC* sites do not appear to be localized to nucleoli or telomeric foci.

Peripheral positioning of *ETC* sites requires the extended *B box* consensus sequence

We next tested whether the extended *B box* consensus (and by extension TFIIIC binding) is required for *ETC*-site perinuclear localization. Starting with the chromosome dot–tagged *ETC6* strain, we deleted the 23–base pair *ETC* consensus along with 10 base pairs of intergenic sequence on either side, resulting in a total deletion of 43 base pairs (illustrated in Figure 3A). No other *B box*–like sequence is present in the intergenes where *ETC6* lies, and this *etc6*Δ mutant no longer binds TFIIIC (Figure 3B).

Deleting the *ETC6* consensus caused the locus to become randomly positioned in all three cell cycle phases (Figure 3, C and D). The *B box* extended *ETC* consensus therefore appears essential for tethering *ETC6* to the nuclear periphery. Analogous data were obtained on deleting the *ETC7* consensus (Supplemental Figure S2, A and B). To summarize, the conserved *B box* extended consensus sequence is critical for perinuclear localization of *ETC* loci.

An *ETC* site can direct peripheral tethering of a random chromosome locus

We examined whether an *ETC* locus inserted at a randomly positioned chromosomal region can direct its localization to the nuclear periphery. We constructed a strain in which an internal chromosomal intergene (*YNL179C-RPS3*; *ChrXIV-302*) was fluorescently tagged and confirmed that this *ChrXIV-302* locus is randomly distributed in the nucleus throughout interphase (Figure 4, A and B). We next inserted at *ChrXIV-302* a 91–base pair fragment of *RAD2-TNA1* intergenic sequence from *ChrVII*, encompassing *ETC4*. Subnuclear localization revealed that the resulting "ectopic" *ETC* site was positioned in zone 1 in the majority of interphase cells (Figure 4C). In contrast, insertion of an *ETC4* fragment containing a mutated consensus sequence incapable of binding TFIIIC (*etc4mut*; Simms *et al.*, 2008) was unable to direct peripheral localization (Figure 4D). An *ETC* site can therefore direct peripheral tethering even if moved to a new chromosomal context, with positioning dependent on an intact TFIIIC-binding consensus. Larger genomic fragments containing *ETC2* or *ETC6* were also able to direct peripheral positioning when inserted at the *ChrXIV-302* site (Supplemental Figure S2, C and D).

Degradation of Tfc3 causes release of an *ETC* site from the periphery

The eight *ETC* sites were discovered on the basis of their TFIIIC occupancy (Moqtaderi and Struhl, 2004). To test directly whether

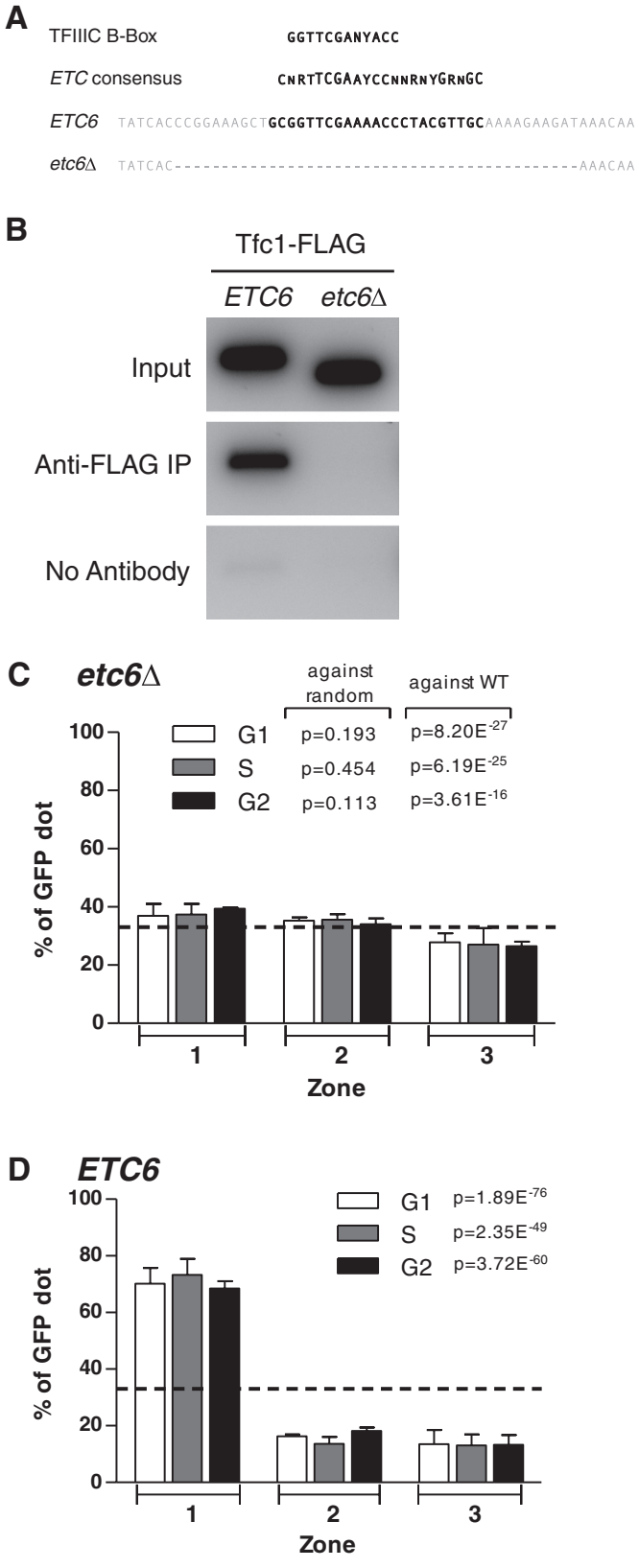

FIGURE 3: The extended *B box* consensus is crucial for peripheral localization of *ETC6*. (A) Sequence comparisons show the TFIIIC-binding *B box* consensus present at tRNA genes, the extended *B box*–related consensus sequence of *ETC* sites, a 55–base pair stretch of the *TFC6-ESC2* intergene containing *ETC6*, and the sequence of the *etc6*Δ strain. (B) The *ETC6* consensus is required for TFIIIC binding. Binding of FLAG-tagged Tfc1 protein to *ETC6* or the *etc6*Δ locus was examined by chromatin immunoprecipitation. Strains are DDY4729 and DDY4732. (C) Intranuclear positioning of the *etc6*Δ locus, plotted as in Figure 1D. (D) Intranuclear positioning of *ETC6*. Dashed black lines indicate the value expected for random localization in these and subsequent graphs. Strains are SBY1, SBY2, and SBY6 (*ETC6*) and SBY37 and SBY38 (*etc6*Δ). Error bars represent SD of values obtained from independent strain isolates (n = 3 for *ETC6*, n = 2 for *etc6*Δ). The p values were calculated by χ^2 analysis in which the observed distribution for *etc6*Δ was compared with either a hypothetical random distribution or to *ETC6*. At least 150 cells were inspected at each cell cycle stage for each strain.

TFIIIC mediates *ETC* site peripheral tethering, we fused an auxin-inducible degron (Nishimura *et al.*, 2009) to Tfc3 in the strain containing the fluorescently tagged *ETC4* locus and tested the effects of inducing Tfc3 degradation on *ETC4* localization. Microscopic examination of cells 1–2 h after addition of the auxin 3-indoleacetic acid (IAA) revealed that *ETC4* peripheral localization was ablated (Figure 5A). In contrast, *ETC4* localization remained largely intact in a control strain with untagged Tfc3 (Figure 5B). The rapid loss of *ETC4* peripheral positioning on induction of Tfc3 degradation suggests that TFIIIC is directly responsible for tethering *ETC* sites at the nuclear periphery.

TFIIIC subunits drive anchoring of a chromosome locus at the nuclear periphery

The foregoing results implicate TFIIIC in the *ETC* tethering mechanism. We therefore tested whether TFIIIC alone can drive tethering of a chromosomal domain to the nuclear periphery. We used a system developed as a cytological assay for proteins that cause peripheral tethering (Taddei *et al.*, 2004; Ebrahimi *et al.*, 2010). Briefly, LexA-binding sites (*lexA*^{Op}) are inserted at a randomly positioned chromosome locus (*ChrVI*^{int}, adjacent to *ARS607* on chromosome VI). Candidate anchoring proteins are expressed fused to the LexA DNA-binding domain and their effect on *ChrVI*^{int} subnuclear position assessed. An array of *lac*^{Op} repeats at the same site allows subnuclear positioning of *ChrVI*^{int} to be monitored microscopically (Figure 6A; Taddei *et al.*, 2004).

We tested the ability of LexA-fused TFIIIC components to cause peripheral localization of *ChrVI*^{int}. Expression of LexA alone does not affect *ChrVI*^{int} localization (Figure 6D), but expression of either LexA-Tfc1 or LexA-Tfc6 induces anchoring of *ChrVI*^{int} to the nuclear periphery (Figure 6, B and C). In both cases, peripheral anchoring levels were highest in G1 and dropped slightly in S and G2 phases. Similar results were obtained on expression of LexA fused to other TFIIIC subunits (LexA-Tfc3, LexA-Tfc4, LexA-Tfc7, and LexA-Tfc8; Supplemental Figure S3).

The fact that all the TFIIIC subunits were able to induce some level of peripheral tethering suggested that binding of one Lex-Tfc protein to DNA might cause recruitment of other TFIIIC subunits. We tested this possibility, and found, using chromatin immunoprecipitation (ChIP) analysis, that binding of LexA-Tfc3 or LexA-Tfc6 causes corecruitment of Tfc1 (Figure 6E). Together with the positioning data, this result suggests that tethering any TFIIIC subunit can cause nucleation of the other complex subunits to direct peripheral localization.

Mps3 is required for *ETC*-locus peripheral anchoring

We aimed to identify the nuclear envelope component responsible for anchoring *ETC* sites at the nuclear periphery. One candidate was Mps3, a Sad1-UNC-84 (SUN)–domain inner nuclear envelope protein. Mps3 functions as an integral membrane anchor for telomeres

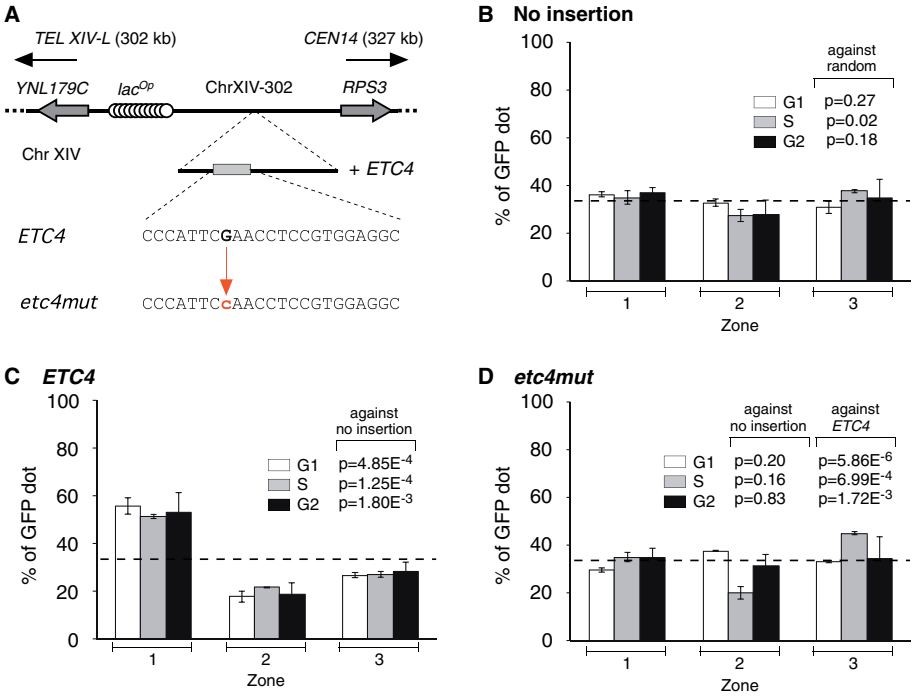

FIGURE 4: An *ETC* site inserted at a randomly positioned locus directs peripheral localization. (A) Illustration of strain construct. Intergene *YNL179C-RPS3*, at 302 kb on the chromosome XIV left arm, was GFP tagged using a *lac*^{Op} array. A 91–base pair fragment of either wild-type *ETC4* or a version of *ETC4* with a single base substitution in its *B box* consensus (*etc4mut*) was inserted as illustrated, and localization was tested. (The total insertion length in both cases was 225 base pairs, with the 91–base pair *ETC4* or *etc4mut* sequences flanked by 23– and 111–base pair sequences derived from plasmid vector at left and right, respectively.) (B) Intranuclear positioning of GFP-tagged *ChrXIV-302* locus, plotted as in Figure 1D. (C) Intranuclear positioning of the *ChrXIV-302* locus with inserted *ETC4*. (D) Intranuclear positioning of the *ChrXIV-302* locus with *etc4mut* insertion. Error bars represent SD of values obtained from three independent strain isolates. The p values were calculated by χ^2 analysis, with observed positioning compared either to *ChrXIV-302* or to a hypothetical random distribution. For the *etc4mut* construction, p values against the inserted *ETC4* were also calculated. Strains were SBY76, SBY77, SBY78 (*ChrXIV-302*), SHY465 (*ChrXIV-302 + ETC4*), and SHY468 (*ChrXIV-302 + etc4mut*). At least 80 cells were inspected at each cell cycle stage for each strain.

(Bupp *et al.*, 2007) and is also involved in sequestering double-strand break sites at the nuclear periphery (Oza *et al.*, 2009). Mps3 is an essential protein, so we examined the impact of a mutant version that lacks the N-terminal nucleoplasmic domain required for localizing telomeres (the previously described *mps3Δ75–150* allele; Bupp *et al.*, 2007).

Deleting this Mps3 N-terminal domain resulted in random positioning of the *ETC6* locus in all three cell cycle phases (Figure 7A), demonstrating that Mps3 is important for anchoring *ETC6* to the nuclear periphery. Similar data were obtained on subnuclear localization analysis of *ETC2* in the *mps3Δ75–150* mutant (Figure 7B). This loss of peripheral anchoring suggests that the SUN-domain protein Mps3, and specifically its N-terminal nucleoplasmic domain, plays an important role in the perinuclear tethering of *ETC* loci.

To exclude the possibility that loss of tethering is an indirect consequence of the *mps3Δ75–150* mutation, we examined the effect of ectopically overexpressing a dominant-negative version of *MPS3* containing only its nucleoplasmic N-terminal domain fused to tetR-mCherry to permit visualization. A similar fusion construct was previously shown to interfere with telomere anchoring at the nuclear periphery (Schober *et al.*, 2009). Microscopic observation revealed that this Mps3-N-tetR-mCherry (Mps3-N′) protein localizes throughout the nucleoplasm (Supplemental Figure S4A), in contrast to full-length Mps3 (Bupp *et al.*, 2007) and as expected, since this Mps3-N′ construct lacks the Mps3 membrane-spanning domain. We found that the overexpression of Mps3-N′ (from a multicopy vector in a wild-type *MPS3* background) ablates peripheral positioning of the *ETC4* locus (Figure 7C). Expression of Mps3-N′ also prevented peripheral positioning of *ETC6* (Supplemental Figure S4B). These results support the conclusion that Mps3, and specifically its N-terminal domain, is involved in *ETC* locus anchoring to the nuclear periphery. We propose that the soluble Mps3 N′ domain competes with full-length, membrane-attached Mps3, preventing proper recruitment of the *ETC4* site to the nuclear periphery and resulting in its random localization within the nuclear space. The finding that overexpressing the Mps3-N′ domain interferes with *ETC*-site peripheral positioning supports the idea that *ETC* nuclear membrane anchoring involves an interaction with the N-terminal domain of Mps3.

Ectopic expression of the Mps3 N-terminus antagonizes TFIIIC-mediated peripheral tethering

Because anchored TFIIIC subunits are central to *ETC* site positioning, we tested whether Mps3-N′ also antagonizes ectopic peripheral tethering driven by TFIIIC components. Using the LexA-based tethering system described previously (Figure 6A), we found that Mps3-N′ overexpression severely compromised the ability of LexA-fused TFIIIC subunits to drive localization to the nuclear rim. Specifically, neither LexA-Tfc7 nor LexA-Tfc1 is effective in anchoring *ChrVI*^{int} when Mps3-N′ is overexpressed (Figure 8 and Supplemental Figure S4, C and D). In contrast, Mps3-N′ did not affect anchoring-mediated Yif1, a nuclear transmembrane protein previously found to cause peripheral tethering (Andrulis *et al.*, 1998). Our observations favor a model in which TFIIIC mediates peripheral tethering of *ETC* sites based on either direct or indirect interactions between TFIIIC and the Mps3 N-terminal domain.

Peripheral tethering is not required for *ETC4* transcriptional insulator and heterochromatin barrier activities

Several *ETC* sites have been shown to function as "insulators" (blocking transcriptional activation by an enhancer) or as "barriers" (interrupting the spread of heterochromatin; Sun and Elgin, 1999; Simms *et al.*, 2008; Valenzuela *et al.*, 2009). To examine whether positioning at the nuclear periphery is required for these *ETC* functions, we tested the effect on *ETC4* insulator and barrier activity of overexpressing the Mps3-N′ domain, which, as shown previously, is a dominant inhibitor of peripheral localization. We used an established assay for enhancer blocking transcriptional insulator activity (Figure 9A; Simms *et al.*, 2008), in which *ETC4* inserted between the *GAL10* ORF and its UAS_G activator sequences prevents *GAL10* transcription and, as a consequence, growth on galactose medium (Figure 9B, lower left quadrant). Growth on galactose was not improved by overexpressing

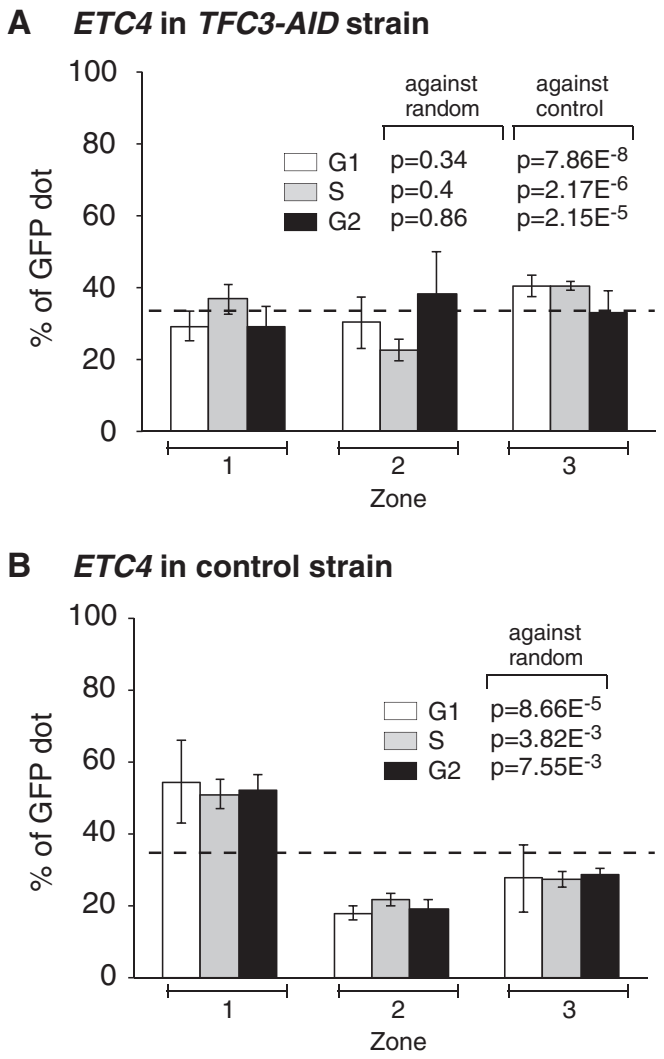

FIGURE 5: TFIIIC plays a critical role in peripheral anchoring of *ETC* sites. (A) Subnuclear positioning of *ETC4* was examined in a strain SHY476 expressing Tfc3 C-terminally tagged with an auxin-inducible degron. Degradation of Tfc3 protein was induced by adding 3-indoleacetic acid, and perinuclear positioning of *ETC4* was examined 1 h later. (B) Subnuclear positioning of *ETC4* was examined in control strain SHY472 that lacks the degron. The p values were calculated by χ^2 analysis in which observed distribution was compared either to a hypothetical random distribution or to that for control strain. At least 50 cells were inspected for each cell cycle stage in each strain.

Mps3-N′ (Figure 9B, lower right quadrant), showing that *GAL10* still fails to be transcribed. This finding suggests that *ETC4* retains insulator activity even when it is not localized at the nuclear periphery. Consistent with this interpretation, *ETC4* also retained insulator function in a strain background in which the Mps3 N-terminal perinuclear domain was deleted (Supplemental Figure S5).

The function of *ETC4* as a barrier to heterochromatin was assessed using the assay construct illustrated in Figure 9C, which tests whether silenced chromatin spreading from the silenced *HMRa* mating locus represses transcription of *ADE2* (Jambunathan *et al.*, 2005; Simms *et al.*, 2008). Reduced *ADE2* transcription results in pink colony pigmentation. The *tRNA* gene (*tDNA*) lying next to *HMRa* provides barrier activity that prevents spread of silent chromatin, allowing efficient *ADE2* transcription and white colony color (Figure 9D, *tDNA* and *tdnaΔ*; left; Donze *et al.*, 1999). Barrier function can be provided by a copy of *ETC4* replacing the *tDNA* but not by a mutated version *etc4mut* (Figure 9D, *ETC4* and *etc4mut*; left). We found that *ETC4* (and the *tDNA*) can still block the spread of heterochromatin when Mps3-N′ is overexpressed, as indicated by the formation of white colonies, implying successful transcription of *ADE2* (Figure 9D, *ETC4* and *tDNA*; right). We conclude that *ETC4* can continue to function as a heterochromatin barrier element even when its peripheral localization is disrupted. We also found that *ETC1*, which is not peripherally localized (Figure 1), is not effective as a transcription-blocking insulator or as a heterochromatin barrier element (Supplemental Figure S6, A and B).

DISCUSSION

ETC loci as *COC* sites

Here we described *S. cerevisiae ETC* sites as a new class of sequence loci positioned at the nuclear periphery. We found that six of eight identified *S. cerevisiae ETC* loci exhibit peripheral localization. *ETC* loci therefore represent distinct chromosome sites conserved in eukaryote genomes, involved in directing correct spatial positioning within the eukaryotic nucleus (Noma *et al.*, 2006). *ETC* sites are not colocalized with telomere foci, nor are they positioned within the nucleolus. Our experiments suggest that TFIIIC bound at *ETC* sites directly mediates their peripheral localization, since mutating its binding site or degrading a TFIIIC subunit abolishes positioning. We find indeed that anchoring TFIIIC subunits at an ectopic chromosomal site can drive localization to the nuclear periphery. Disrupting function of the Mps3 N-terminal domain prevents *ETC*-site localization, but *ETC* site chromatin boundary function remains intact.

Our results clearly implicate TFIIIC as central for the *ETC*-site positioning mechanism, a finding that raises interesting questions about the involvement of the RNA Pol III apparatus in spatial organization of the genome. Active Pol III–transcribed tRNA genes appear preferentially localized to the nucleolus (Thompson *et al.*, 2003), but we found no significant colocalization of either *ETC5* or *ETC7* with the nucleolus. It has been suggested that another category of tRNA genes may tend to colocalize with centromeres (Duan *et al.*, 2010), but we saw no tendency for *ETC* sites to associate with centromeres or telomere clusters. Perinuclear anchoring of *ETC* sites therefore appears to represent a new mode of TFIIIC-mediated positioning, acting aside from and independent of nucleolar and telomere localization. The fact that *ETC*-site peripheral localization is retained throughout interphase also differs from previously described peripheral positioning mechanisms. In particular, *ETC* sites do not appear to undergo the replication-triggered release from the nuclear periphery that leads to delocalization of telomeres during G2 (Ebrahimi and Donaldson, 2008).

ETC sites all contain an extended *B box* sequence that is conserved among sensu stricto *Saccharomyces* species (Moqtaderi and Struhl, 2004). Deletion of the *B box* extended consensus and immediately surrounding sequence ablated tethering of the *ETC7* and *ETC6* sites to the nuclear envelope, showing that the TFIIIC binding sequence is required for tethering, in agreement with studies in *S. pombe* (Noma *et al.*, 2006). Moreover, a version of *ETC4* mutated in its TFIIIC-binding consensus was unable to cause localization of an ectopic site. One possibility is that the variant, extended *B box* consensus present at *ETC* sites may allow TFIIIC to direct peripheral localization rather than TFIIIB recruitment, perhaps by altering its mode of binding.

We addressed the importance of the *B box*–based consensus by moving *ETC* loci to a new chromosomal context. All three loci tested (*ETC4*, *ETC2*, and *ETC6*) can direct peripheral tethering even in a

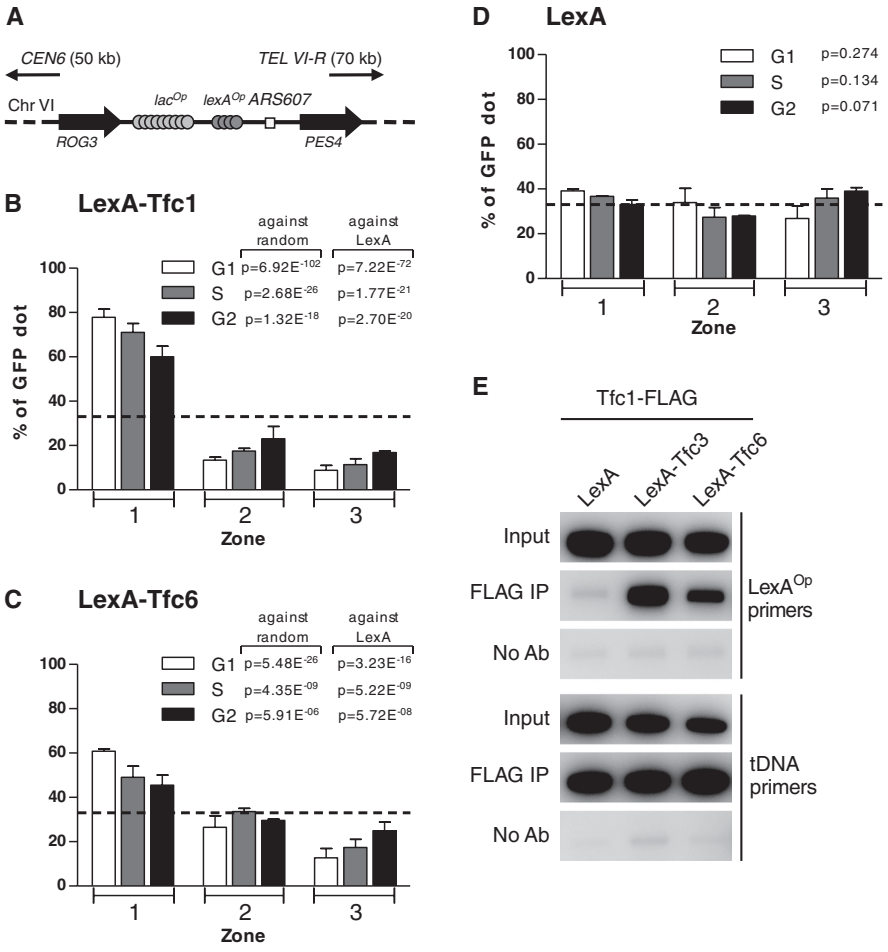

FIGURE 6: TFIIIC subunits can mediate peripheral anchoring. (A) Illustration of *ChrVI*^{int} locus in tethering assay strain. In addition to *lac*^{Op} repeats, an array of four *lexA*^{Op}-binding sites is inserted at 199.2 kb on the chromosome VI right arm, adjacent to replication origin *ARS607* (Taddei *et al.*, 2004). (B) Positioning of *ChrVI*^{int} induced by LexA-Tfc1, tested as in Figure 1D. (C) Positioning of *ChrVI*^{int} induced by LexA-Tfc6. (D) Positioning of *ChrVI*^{int} when LexA is expressed. Strains were GA1461 (LexA); SBY155, SBY156 (LexA-Tfc1); and SBY144 and SBY146 (LexA-Tfc6). Error bars represent SD of values obtained from independent strain isolates (n = 2). The p values were calculated by χ^2 analysis in which observed distribution was compared either to a hypothetical random distribution or to distribution on expression of LexA. At least 130 cells were inspected for each strain at each cell cycle stage. (E) LexA-Tfc3 and LexA-Tfc6 subunit fusions recruit Tfc1 to ectopic *lexA*^{Op}-binding sites. Binding of FLAG-tagged Tfc1 protein close to *lexA*^{Op} sites was examined by chromatin immunoprecipitation in strains expressing LexA or the fusion protein LexA-Tfc3 or LexA-Tfc6. The anti-FLAG chromatin immunoprecipitates show enrichment for sequences surrounding the *lexA*^{Op} sites when LexA-Tfc3 or LexA-Tfc6 is expressed but not when LexA alone is expressed. Amplification of an unrelated tRNA gene sequence (tDNA) shown as a Tfc1-binding control locus. Strains are SHY459, SHY461, and SHY463.

new chromosomal context, with retention of peripheral positioning throughout interphase (as at endogenous *ETC* loci). Our results support the suggestion that TFIIIC binding alone is enough to drive peripheral localization, overriding other limitations presented by chromatin context. It is notable that *ETC1* and *ETC3*, the two sites that display little or no peripheral localization, displayed the lowest TFIIIC binding in the study that originally identified the *S. cerevisiae ETC* loci (Moqtaderi and Struhl, 2004), and *ETC3* has the weakest homology to the *B box* consensus. A role for TFIIIC as a major component in the positioning mechanism is further suggested by our finding that artificial recruitment of TFIIIC subunits mediates peripheral anchoring of a randomly positioned locus (Figure 6).

Examining other candidate molecular components that could mediate *ETC*-site peripheral tethering led us to identify the SUN-domain inner nuclear membrane protein Mps3 as a possible nuclear envelope anchor. Mps3 is a multifunctional protein previously found to act in spindle pole duplication, telomere peripheral tethering, and localization of DNA-break sites (Bupp *et al.*, 2007; Schober *et al.*, 2009). Deletion of the Mps3 N-terminal domain (*mps3Δ75-150*) severely compromised tethering to the nuclear envelope of two different *ETC* loci (*ETC6* and *ETC2*). Mps3 may function as the *ETC* perinuclear anchor through its N-terminal acidic domain, which is located within the nucleoplasm and could interact with TFIIIC. Overexpressing a soluble N-terminal fragment of Mps3 in an *MPS3* wild-type background ablated the perinuclear tethering of *ETC* loci and prevented LexA-Tfc–driven peripheral tethering of the *ChrVI*^{int} locus (Figure 8 and Supplemental Figure S4, A and B), suggesting that Mps3-N′ competes with endogenous Mps3 for *ETC*-site interaction. These results support the idea that Mps3 acts as the *ETC* perinuclear anchor protein through its N-terminal nucleoplasmic domain. However, coimmunoprecipitation and two-hybrid tests did not reveal a direct interaction between Mps3 and any TFIIIC subunit (unpublished data), so we cannot exclude the possibility that the effect of Mps3 on *ETC*-site positioning is indirect and involves additional, unidentified components. We tested the effect of the variant histone Htz1, since Mps3 has been shown to interact with Htz1 (Gardner *et al.*, 2011) and Htz1 is incorporated close to some *ETC* sites (Albert *et al.*, 2007). Deleting Htz1, however, had only a marginal effect on *ETC* site positioning (unpublished data).

We previously found that *ETC*-site peripheral tethering required the activity of chromatin-remodeling proteins and in particular H3-K56 acetylation (Hiraga *et al.*, 2008). Proteins like Yku70/Yku80 and Sir4, which are involved in telomere peripheral anchoring pathways, in contrast have only a marginal effect on *ETC6* peripheral positioning (Hiraga *et al.*, 2008). Further work will be required for a complete understanding of the *ETC*-anchoring pathway and identification of any additional protein components involved.

What is the function of *ETC* sites?

The conservation of *ETC*-site consensus sequences throughout sensu stricto *Saccharomyces* species suggests an important biological function for these loci. Six of the eight *S. cerevisiae ETC* loci lie between divergently transcribed genes, similar to the arrangement of most *COC* sites in *S. pombe* (Noma *et al.*, 2006). *ETC* sites can behave as chromatin boundary elements, but copy number expression data (Ghaemmaghami *et al.*, 2003) reveal no particular tendency for

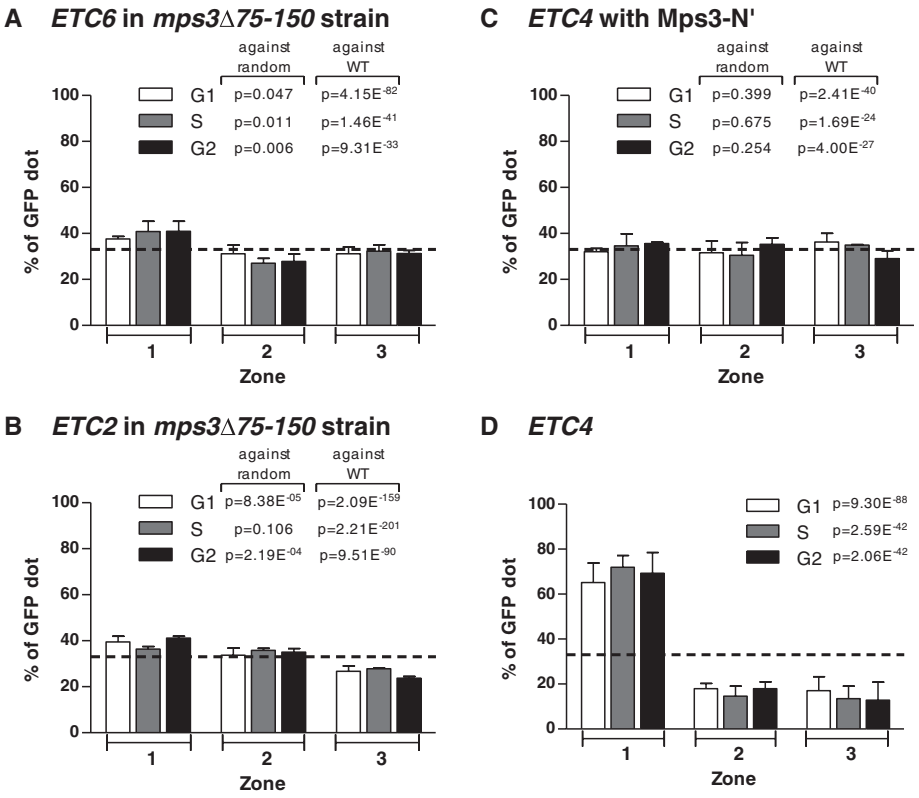

FIGURE 7: An Mps3 N-terminal domain plays a role in peripheral anchoring of *ETC* sites. (A) Subnuclear positioning of *ETC6* in *mps3Δ75-150* strain was tested as in Figure 1D. Strain is SBY191. *ETC6* positioning in wild type is shown in Figure 3. (B) Subnuclear positioning of *ETC2* in *mps3Δ75-150* strain. Strain is SBY195. *ETC2* positioning in wild type is shown in Figure 1. (C) Subnuclear localization of *ETC4* in strain expressing Mps3-N′-tetR-mCherry (Mps3-N′) from a multicopy vector. (D) Normal subnuclear localization pattern of *ETC4*, shown for reference. Strains used were SBY196 (*ETC6*; *mps3Δ75-150*); SBY194, SBY197, and SBY198 (*ETC2*; *mps3Δ75-150*); SBY217 and SBY218 (Mps3-N′); and SBY21, SBY22, and SBY23 (wild type). Error bars represent SD of values obtained from independent strain isolates (n = 3 for data presented in A, B, and D; n = 2 for C). The p values were calculated by χ^2 analysis in which observed distribution was compared either to a hypothetical random distribution or to that for normal *ETC* localization. At least 160 cells were inspected at each cell cycle stage for each strain.

genes flanking *ETC* sites to be expressed at very different levels. There is a slight enrichment for genes within in the lowest 5% of expression levels in the vicinity of *ETC* sites (within the five flanking genes to the left and right). *ETC* sites might therefore tend to be associated with transcriptional suppression, but the significance of this observation is marginal, with the low number of identified sites limiting statistically significant conclusions. At least one *S. pombe COC* site behaves as a boundary element to limit the spread of silenced chromatin, and it was suggested that peripheral tethering of *COC* sites might facilitate boundary activity by creating a barrier to processive assembly of heterochromatin (Noma *et al.*, 2006). However, we found that *ETC4* retained both heterochromatin barrier and transcription-blocking insulator functions even under conditions in which *ETC*-site peripheral localization is ablated (Figure 9 and Supplemental Figure S5), implying that perinuclear localization is not required for these activities. Consistent with our observations, a recent study found although nuclear pore proteins associate with a tRNA gene barrier element at a modified HMRa locus, pore protein association is not essential for barrier activity (Ruben *et al.*, 2011). The biological significance of *ETC*-site peripheral positioning is unclear, although one interesting possibility is of a relationship to condensin function, since the Pol III apparatus has been implicated in recruiting condensin to *S. cerevisiae* chromosomes (D'Ambrosio *et al.*, 2008; Haeusler *et al.*, 2008) and condensin is localized to a subset of the *ETC* sites. It will be interesting to explore further the relation between condensin, *ETC*-site function, and localization at the nuclear periphery.

The recent discovery of large numbers of *ETC* loci in the human and mouse genomes represents a particularly interesting addition to our knowledge of *ETC/COC* loci and reinforces the suggestion of additional roles for eukaryotic TFIIIC beyond its function in Pol III transcription (Simms *et al.*, 2008; Moqtaderi *et al.*, 2010; Carriere *et al.*, 2012). The large number of mammalian *ETC* loci raises the question of whether additional *ETC* sites exist in the *S. cerevisiae* genome. Two recent studies hinted there may be uncharacterized TFIIIC-binding sites in *S. cerevisiae* (D'Ambrosio *et al.*, 2008; Venters *et al.*, 2011), which have yet to be validated or further investigated. Some of the human *ETC* sites contained a novel motif (instead of the known TFIIIC-binding motif), so it is even possible that additional yeast *ETC* sites might not contain a TFIIIC-binding consensus. Like yeast *ETC* sites, human *ETC* loci also tend to lie in closely spaced, divergently transcribed Pol II intergenic regions, hinting that human *ETC* loci could also act as chromatin boundary elements. Human *ETC* loci tend to occur near binding sites for CTCF, a protein implicated in higher-order organization of metazoan chromosomes through cohesin interaction, insulator function, and chromosome looping (Wallace and Felsenfeld, 2007; Parelho *et al.*, 2008). Overall, the emerging evidence points toward an important role for *ETC* loci in chromosome spatial organization that is conserved throughout eukaryotes.

MATERIALS AND METHODS

Yeast strains and plasmids

All yeast strains were constructed in the W303-1A background (*ade2-1 trp1-1 leu2-3112 ura3-1 his3-11,15 can1-100*). Strains are listed in Supplemental Table S1. Plasmids are listed in Supplemental Table S2. Standard techniques were used for DNA and yeast manipulations.

To tag each *ETC* locus with GFP, a suitable restriction site was identified in the genomic DNA near the *ETC* locus to be tagged. Primers were designed to amplify a ~400–base pair fragment containing this restriction site, and the fragment was cloned into *lac^{Op}* repeat plasmid pAFS52 (Robinett *et al.*, 1996). The resulting plasmid was cut at the unique restriction enzyme site and transformed into yeast strain GA-1320 (Heun *et al.*, 2001), creating strains SBY1-SBY14 and SBY17-SBY25. In the cases of *ETC1*, *ETC4*, *ETC5*, and *ETC8* the size of the intergene allowed the insertion of *lac^{Op}* tagging sequences within the intergene occupied by the *ETC* site (Table 1); for *ETC3*, *ETC6*, and *ETC7* the tag was inserted in a neighboring intergene. Table 1 shows *ETC*-site coordinates,

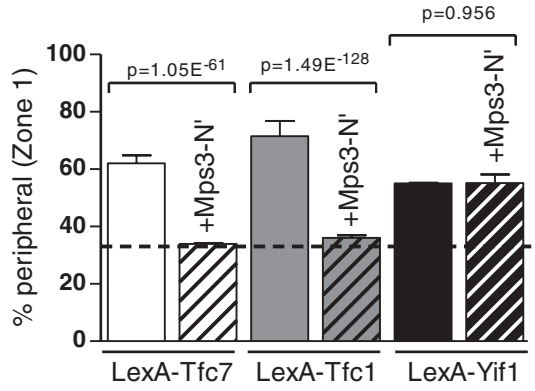

FIGURE 8: Mps3-N′ expression antagonizes peripheral anchoring by TFIIIC subunits. Tethering of *ChrVI*^{int} in strains expressing LexA-Tfc7, LexA-Tfc1, and LexA-Yif1 (white, gray, and black bars respectively) compared with the same strains expressing Mps3-N′ from a multicopy vector (striped white, striped gray, and striped black bars respectively). Percentages of interphase cells showing peripheral (zone 1) positioning of *ChrVI*^{int} are plotted (i.e., cumulative total of G1-, S-, and G2-phase cells). Strains used were SBY148, SBY149 (LexA-Tfc7); SBY155, SBY156 (LexA-Tfc1); SBY211, SBY212 (LexA-Yif1); SBY219, SBY220 (LexA-Tfc7 + Mps3-N′); SBY221, SBY222 (LexA-Tfc1 + Mps3-Nz); and SBY223 and SBY224 (LexA-Yif1 + Mps3-Nz). Error bars represent SD of values obtained from independent strain isolates (n = 2). The p values were calculated by χ^2 analysis in which observed distribution was compared either to a hypothetical random distribution or to distribution in the absence of Mps3-N′.

ETC-site sequences, and relative distances of the *lac*^{Op} insert from the *ETC* locus.

To test for *ETC* colocalization with the nucleolus, we tagged the endogenous *NOP1* gene with mCherry (Shu *et al.*, 2006). Briefly, SBY3 and SBY13 were transformed with a DNA fragment containing the *natMX4* marker and *mCherry* targeted for in-frame insertion at the *NOP1 3′* end, creating strains SBY31-33 and SBY49-51. To test for colocalization of *ETC* sites with telomeres, strains SBY84-86 and SBY87-89 were made by transforming SBY3 and SBY10, respectively, with plasmid pSB33 (YCp-*mCherry-RAP1*). The pSB33 plasmid resulted from exchanging GFP with mCherry (pKT355; Iwase *et al.*, 2006) in plasmid YCp-*GFP-RAP1* (Hiraga *et al.*, 2006).

Strains SBY26, SBY27 (*etc7*Δ), and SBY37, SBY38 (*etc6*Δ) were derived from SBY3 and SBY1, respectively, by deleting the 23–base pair extended *B box* consensus sequence (23 base pairs) and 10 flanking base pairs on either side (43 base pairs total) using a fragment lacking this 43–base pair sequence but having 40–base pair homology on each side to the sequences flanking the deletion. This was performed in two steps. First the *URA3* marker gene (YDp-U; Berben *et al.*, 1991) was inserted at the appropriate *ETC* site, followed by disruption with either the *etc6*Δ or *etc7*Δ deletion fragment and selection of correct isolates by plating cells to 5-fluoroorotic acid. To create strains for Tfc1-FLAG ChIP (Figure 3B), we crossed SBY1 and SBY37 with DDY4058 and sporulated them to produce DDY4729 and DDY4732.

To insert an *ETC* site on another chromosome, we selected a suitable chromosomal locus (*ChrXIV: RPS3-YNL179C* intergene) and GFP tagged it (as described previously), creating SBY76, SBY77, and SBY78. A DNA fragment containing a *kanMX* marker flanked by *loxP* sites and a ~450–base pair sequence containing either *ETC2* or *ETC6* was targeted for integration next to the GFP tag. Removal of the *kanMX* marker by expressing Cre recombinase from a pSH47 plasmid (Guldener *et al.*, 1996) then created SBY135, SBY136, and SBY137 and SBY139, SBY142, and SBY143. For transfer of *ETC4*, double-stranded synthetic oligonucleotides containing wild-type *ETC4* or a mutated version of *ETC4* with a single base substitution in *B box* consensus (*etc4mut*; Simms *et al.*, 2008) were cloned in between *Bam*HI and *Sal*I sites of plasmid pU6H3FLAG (Katou *et al.*, 2003). The resulting plasmids pSH136 and pSH138 contain wild type or *etc4mut* adjacent to loxP-kanMX-loxP, respectively. PCR fragments containing *ETC4* and loxP-kanMX-loxP were PCR amplified with primers (with genomic sequence of chrXIV-302 at their 5′ ends) and used to transform strain SBY76. After insertion of *ETC4*

ETC locus (intergene)	Sequence	Chromosome coordinates	Distance from closest telomere (kb)	GFP-tagged intergene	Distance of *Lac*^{Op} from center of *ETC* (kb)
ETC1 (*ADE8-SIZ1*)	CTCATTCGAATCCT-TGCTGACGC	ChrIV: 1289041–1289063	243	*ADE8-SIZ1*	9.0
ETC2 (*PPM2-ARG8*)	GCTCCTATCGG-GATTCGAATGGT	ChrXV: 58541–58563	59	*ARG8-CDC33*	6.6
ETC3 (*MAPL49- BCK1*)	GCCATTCAATTCCA-GACCGACGC	ChrX: 247060–247082	247	*SAP185-PHS1*	10.4
ETC4 (*RAD2-TNA1*)	GCCTCCACGGAG-GTTCGAATGGG	ChrVII: 1010927–1010949	80	*RAD2-TNA1*	5.7
ETC5 (*RNA170*)[a]	GCTCCAGGGCA-GAATCGAACCAC	ChrXIII: 667324–667346	257	*RAD14-ERG2*	9.3
ETC6 (*TFC6-ESC2*)	GCAACGTAG-GGTTTTCGAACCGC	ChrIV: 1198885–1198907	333	*BCP1-TFC6*	11.2
ETC7 (*YOR228C-WTM2*)	GCCCCGTTCG-GGGTTCGAACTGC	ChrXV: 768106– 768128	323	*WTM2-WTM1*	7.2
ETC8 (*RPB5-CNS1*)	GCCTCCGTTAG-GAGTCGAATAGA	ChrII: 549229–549251	264	*RPB5-CNS1*	9.1

[a]*ETC5* locus resides in the coding region of the *RNA170* gene, which is found in the intergene between *RAD14* and *ERG2*.

TABLE 1: *ETC* loci and GFP tagging.

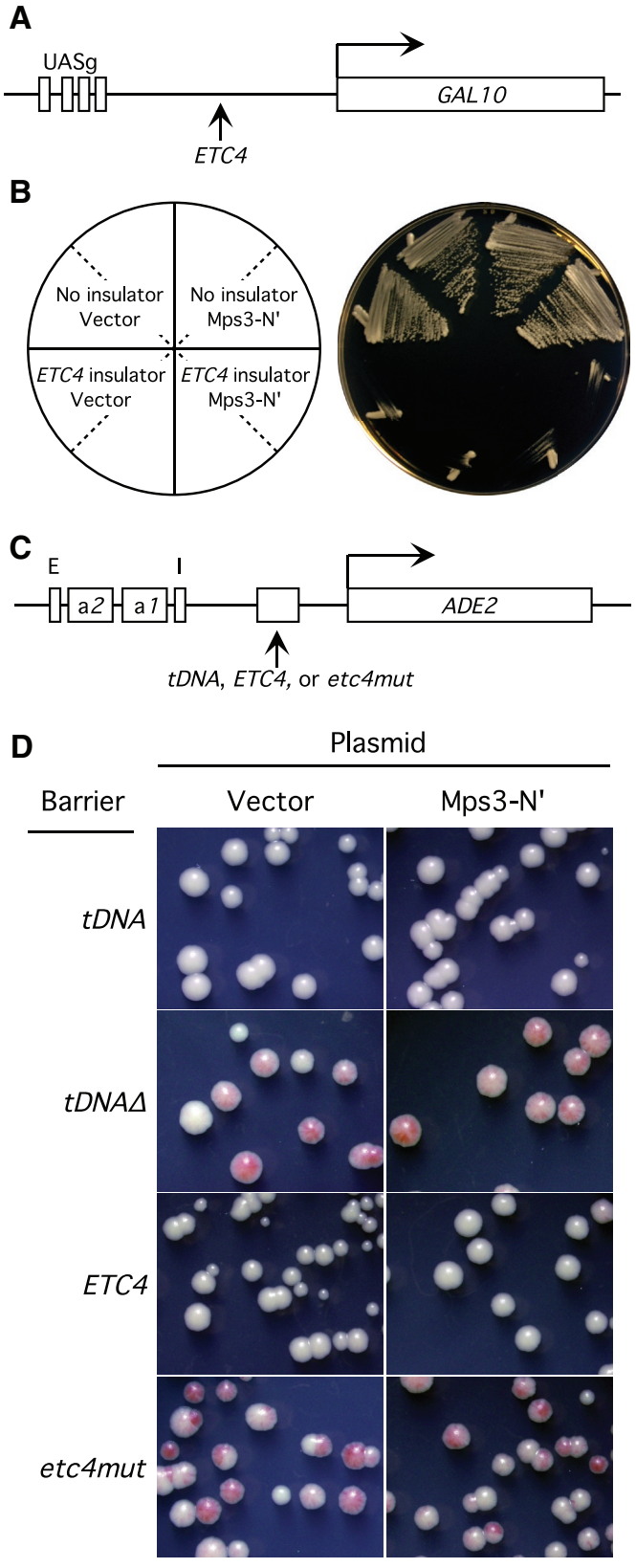

FIGURE 9: *ETC4* transcriptional insulator and barrier activities are not affected by expressing the dominant-negative Mps3-N′ construct that inhibits Mps3-mediated localization. (A) Cartoon of test construct. *ETC4* inserted between the *GAL10* gene and its upstream UAS_G control sequences acts as an insulator and prevents transcriptional activation. (B) *ETC4* insulator activity prevents growth on galactose medium (bottom left quadrant), and expression of Mps3-N′ does not relieve this effect (bottom right quadrant). Strains are DDY3 and DDY3770, transformed with plasmids pRS426 (vector) or pSB79 (Mps3-N′). (C) *HMR*-based chromatin barrier test construct. Spreading of heterochromatin from *HMR* causes transcriptional repression of reporter gene *ADE2*. The neighboring *tDNA* provides barrier activity to prevent the spread of silent chromatin; deleting this *tDNA* results in heterochromatin spreading, causing pink colonies. Barrier activity is retained if the *tDNA* is substituted by *ETC4* (but not a mutated version, *etc4mut*) (D) Expressing dominant-negative Mps3-N′ does not interfere with chromatin barrier function of *ETC4*. Colony color assays of strains with *tDNA*, *tdnaΔ*, *ETC4*, or *etc4mut*, containing either empty vector (left) or the Mps3-N′ plasmid pSB79 (right). Chromatin barrier activity allows *ADE2* expression and white colony color, whereas strains lacking barrier function exhibit pink or red colony color. Strains are DDY811, DDY814, DDY3743, and DDY3812, transformed with plasmid pRS426 (vector) or pSB79 (Mps3-N′).

sequences, the kanMX marker was removed using galactose-inducible Cre recombinase of the plasmid pSH47. The resulting strains SHY465 and SHY468 have a 225–base pair sequence inserted at the chrXIV-302 locus containing *ETC4* or *etc4mut*, respectively.

All LexA fusions were created in pAT4 (Taddei *et al.*, 2004). Fusion proteins were created by inserting the full-length sequences of *TFC1*, *TFC3*, *TFC4*, *TFC6*, *TFC7 (YOR110W)*, or *TFC8* (made by PCR amplification) into pAT4. Error-free constructs were confirmed by sequencing, and the resulting plasmids were then used to transform strain GA-1461 (Hediger *et al.*, 2002) to create SBY144-149, SBY155-166, and SBY211-212.

To construct strains suitable for ChIP analysis of Tfc1-FLAG recruitment by LexA-Tfc fusions, first we cloned double-stranded synthetic DNA containing four LexA operator sequences between the *Bsi*WI and *Sal*I site of plasmid pUG27 to obtain plasmid pSH142. Using pSH142 as a PCR template, we inserted the LexA operator array near the *ARS607* locus of DDY4071 by one-step PCR replacement to obtain SHY451. The HIS3MX maker was then removed by Cre recombinase to obtain strain SHY457. Strain SHY457 was transformed with a plasmid pAT4, pSB48, or pSB50 to obtain strain SHY459, SHY461, or SHY463, respectively.

Strains SBY191, SBY195, and SBY196 (*ETC6*; *mps3Δ75-150*) and SBY194, SBY197, and SBY198 (*ETC2*; *mps3Δ75-150*) were derived from SBY1 and SBY10, respectively, by directing integration of *Bst*EII-digested pSJ519 plasmid (*mps3Δ75-150*; Bupp *et al.*, 2007) at the chromosomal *LEU2* locus, followed by deletion of the chromosomal copy of *MPS3* using a *natMX4* cassette amplified from strain SLJ2059 (Bupp *et al.*, 2007). Single-copy integration was verified by Southern blotting. Plasmid pSH129 was constructed by recloning the *Bam*HI-*Sal*I fragment of pSJ148 (bearing the *MPS3* gene) into *Bam*HI-*Sal*I–cut pRS316.

The Mps3-N-tetR-mCherry construct, pSB79, was created in a pRS426 backbone through three steps of ligation. The promoter region and N-terminal domain of *MPS3* N-terminal domain containing residues 1–151 of *MPS3* were amplified from pSJ148 plasmid (Bupp *et al.*, 2007) using primers that incorporated the *Xho*I and *Aat*II, *Eco*RI restriction sites at the 5′ and 3′ ends of the fragment, respectively. The tetR coding region, flanked by SV40 NLS at its N-terminal end, was amplified from p3524 plasmid (Michaelis *et al.*, 1997) using primers that incorporated the *Aat*II and *Nhe*I, *Spe*I restriction sites, whereas the coding region and termination sequence for mCherry were amplified from pKT355 plasmid (Iwase *et al.*, 2006) using primers that incorporated the *Nhe*I and *Not*I restriction sites. Initial ligation of *Mps3-N′* under its own promoter using the *Xho*I and *Eco*RI restriction sites was followed by in-frame ligation of *tetR* using the *Aat*II and *Spe*I restriction sites and concluded with

in-frame ligation of *mCherry* and *ADH*^{ter} to the existing *Mps3-N-tetR* fusion using the *Nhe*I and *Not*I restriction sites. Strains SBY215, SBY216 (*ETC6*; Mps3-N′); SBY217, SBY218 (*ETC4*; Mps3-N′); SBY219, SBY220 (LexA-Tfc7; Mps3-N′); SBY221, SBY222 (LexA-Tfc1; Mps3-N′); and SBY223, SBY224 (LexA-Yif1; Mps3-N′) were derived from SBY1, SBY22, SBY147, SBY155, and SBY212, respectively, by transforming the aforementioned strains with the multicopy plasmid pSB79 (pRS426-*Mps3-N′-tetR-mCherry*).

To test for correct homologous insertion and replacement events, suitable PCR amplification reactions were designed to analyze the junction sites. *ETC*-site deletions, LexA fusions, and pSB79 (Mps3-N′) construct were confirmed by sequencing.

Insulator assays were as described (Simms *et al.*, 2008) and barrier assays as in Jambunathan *et al.* (2005). Strains to test *ETC1* barrier and insulator activity (Supplemental Figure S6) were constructed as described (Simms *et al.*, 2008).

Auxin-inducible degron

To make strains for the auxin-inducible degradation experiments, the *OsTIR1* gene was inserted into the genomic *URA3* locus of strain SBY22 as described (Nishimura *et al.*, 2009) to obtain strain SHY472. To obtain strain SHY476, an auxin-inducible degron was added to the C-terminus of the genomic copy of the *TFC3* gene in SHY472 as described (Nishimura *et al.*, 2009). Strains SHY472 and SHY476 were cultivated in synthetic raffinose medium buffered at pH5.5 with appropriate auxotrophic selection. At OD_{600} = 0.2–0.3, galactose was added to a final concentration of 2%. One hour after addition of galactose, IAA (Sigma-Aldrich, St. Louis, MO I2886) was added to a final concentration of 0.5 mM. Cells were examined for *ETC4* localization between 1 and 2 h after the addition of IAA.

Chromatin immunoprecipitation

Chromatin immunoprecipitation assays were performed essentially as described (Rusche *et al.*, 2002).

Primers

Primers used to assess TFIIIC binding at *ETC6* and *etc6*Δ delete loci (Figure 3B) were as follows:

DDO-705 (ATTATTACACGTATCGCAATGG) and

DDO-706 (CTATTTCAATTGCGATATACGC)

Primers used to assess binding to *lexA*^{Op} sequences (Figure 6E) were as follows:

DDO-1460 (AAGAAAAAGGGATAAATGCAATG) and

DDO-1461 (CTGACTCTTTTCAACAATGCAG).

The primers for the control tDNA R (CCG) on chromosome XII were as follows:

DDO-1402 (TACGACATCAAAGTCGCCGAG)

DDO-1403 (ATTGACAGCCCTTACGCGAAG)

Other primer sequences are available upon request.

Cytological techniques

Microscopic techniques were performed as described in Hiraga *et al.* (2006). Briefly, a DeltaVision RT (Applied Precision, Issaquah, WA) microscope system with an UPlanApo 100× objective (1.35 numerical aperture; Olympus, Center Valley, PA), CoolSnap HQ monochrome cooled charge-coupled device camera (Photometrics, Tucson, AZ), and SoftWoRx (Applied Precision) acquisition software were used to acquire images. For observation of GFP and *mCherry* fluorescence, 30 Z-stack images were taken at 250-nm intervals with fluorescein isothiocyanate and tetramethylrhodamine isothiocyanate or DsRed filter sets. Differential interference contrast (DIC) images acquired at the same Z-intervals were used for determination of cell cycle stages by bud size: G1 phase, unbudded; S phase, cells with bud ≤2 μm; G2 phase, cells with a bud >2 μm and a spherical (i.e., nonmitotic) nucleus not at the bud neck.

Quantitative evaluation of GFP-tagged chromosomal dot localization was performed as described (Taddei *et al.*, 2004). SoftWoRx Explorer (Applied Precision) was used to measure dot-to–nuclear envelope distance in yeast cells where the GFP dot was located within one of the three equatorial sections of its nucleus. Briefly, localization of the GFP dot was scored in two dimensions against three imaginary concentric zones of equal area, as shown in Figure 1B. At least 300 cells were scored for each isolate measurement (unless otherwise noted). p values were calculated by χ^2 test against either random distribution or wild-type values.

Quantitative evaluation of GFP-tagged chromosomal dot colocalization either with the nucleolus or telomere foci was performed as follows. SoftWoRx Explorer was used to measure dot-to-nucleolus or dot-to-telomere foci distance in yeast cells. Briefly, colocalization of the GFP dot to either the nucleolus or telomere foci was scored in two dimensions if the two structures coincided or were juxtaposed (distance <0.26 μm) when observed within the equatorial region of a Z-stack of images (Figure 5, A and B). At least 200 cells were scored for each isolate measurement (unless otherwise noted). p values were calculated by χ^2 test against random distribution.

ACKNOWLEDGMENTS

We thank all the members of the Donaldson group for comments and technical advice. We thank Sue Jaspersen and Susan Gasser for providing strains and constructs. S.B. was funded by a University of Aberdeen Scholarship. This research was supported by Wellcome Trust Grant 082377/Z/07/Z to A.D. and National Science Foundation Grant MCB-0817823 to D.D.

REFERENCES

Albert I, Mavrich TN, Tomsho LP, Qi J, Zanton SJ, Schuster SC, Pugh BF (2007). Translational and rotational settings of H2A.Z nucleosomes across the *Saccharomyces cerevisiae* genome. Nature 446, 572–576.

Andrulis ED, Neiman AM, Zappulla DC, Sternglanz R (1998). Perinuclear localization of chromatin facilitates transcriptional silencing. Nature 394, 592–595.

Baker RE, Gabrielsen O, Hall BD (1986). Effects of tRNATyr point mutations on the binding of yeast RNA polymerase III transcription factor C. J Biol Chem 261, 5275–5282.

Bartholomew B, Kassavetis GA, Braun BR, Geiduschek EP (1990). The subunit structure of *Saccharomyces cerevisiae* transcription factor IIIC probed with a novel photocrosslinking reagent. EMBO J 9, 2197–2205.

Belgareh N, Doye V (1997). Dynamics of nuclear pore distribution in nucleoporin mutant yeast cells. J Cell Biol 136, 747–759.

Berben G, Dumont J, Gilliquet V, Bolle PA, Hilger F (1991). The YDp plasmids: a uniform set of vectors bearing versatile gene disruption cassettes for *Saccharomyces cerevisiae*. Yeast 7, 475–477.

Bertrand E, Houser-Scott F, Kendall A, Singer RH, Engelke DR (1998). Nucleolar localization of early tRNA processing. Genes Dev 12, 2463–2468.

Brickner JH, Walter P (2004). Gene recruitment of the activated INO1 locus to the nuclear membrane. PLoS Biol 2, e342.

Bupp JM, Martin AE, Stensrud ES, Jaspersen SL (2007). Telomere anchoring at the nuclear periphery requires the budding yeast Sad1-UNC-84 domain protein Mps3. J Cell Biol 179, 845–854.

Carriere L *et al*. (2012). Genomic binding of Pol III transcription machinery and relationship with TFIIS transcription factor distribution in mouse embryonic stem cells. Nucleic Acids Res 40, 270–283.
Casolari JM, Brown CR, Drubin DA, Rando OJ, Silver PA (2005). Developmentally induced changes in transcriptional program alter spatial organization across chromosomes. Genes Dev 19, 1188–1198.
Chung HM, Shea C, Fields S, Taub RN, Van der Ploeg LH, Tse DB (1990). Architectural organization in the interphase nucleus of the protozoan *Trypanosoma brucei*: location of telomeres and mini-chromosomes. EMBO J 9, 2611–2619.
Croft JA, Bridger JM, Boyle S, Perry P, Teague P, Bickmore WA (1999). Differences in the localization and morphology of chromosomes in the human nucleus. J Cell Biol 145, 1119–1131.
D'Ambrosio C, Schmidt CK, Katou Y, Kelly G, Itoh T, Shirahige K, Uhlmann F (2008). Identification of *cis*-acting sites for condensin loading onto budding yeast chromosomes. Genes Dev 22, 2215–2227.
Dawe RK, Sedat JW, Agard DA, Cande WZ (1994). Meiotic chromosome pairing in maize is associated with a novel chromatin organization. Cell 76, 901–912.
de Lange T (1992). Human telomeres are attached to the nuclear matrix. EMBO J 11, 717–724.
Dieci G, Fiorino G, Castelnuovo M, Teichmann M, Pagano A (2007). The expanding RNA polymerase III transcriptome. Trends Genet 23, 614–622.
Donze D, Adams CR, Rine J, Kamakaka RT (1999). The boundaries of the silenced HMR domain in *Saccharomyces cerevisiae*. Genes Dev 13, 698–708.
Duan Z, Andronescu M, Schutz K, McIlwain S, Kim YJ, Lee C, Shendure J, Fields S, Blau CA, Noble WS (2010). A three-dimensional model of the yeast genome. Nature 465, 363–367.
Dujon B (1998). European Functional Analysis Network (EUROFAN) and the functional analysis of the *Saccharomyces cerevisiae* genome. Electrophoresis 19, 617–624.
Ebrahimi H, Donaldson AD (2008). Release of yeast telomeres from the nuclear periphery is triggered by replication and maintained by suppression of Ku-mediated anchoring. Genes Dev 22, 3363–3374.
Ebrahimi H, Robertson ED, Taddei A, Gasser SM, Donaldson AD, Hiraga S (2010). Early initiation of a replication origin tethered at the nuclear periphery. J Cell Sci 123, 1015–1019.
Finlan LE, Sproul D, Thomson I, Boyle S, Kerr E, Perry P, Ylstra B, Chubb JR, Bickmore WA (2008). Recruitment to the nuclear periphery can alter expression of genes in human cells. PLoS Genet 4, e1000039.
Funabiki H, Hagan I, Uzawa S, Yanagida M (1993). Cell cycle-dependent specific positioning and clustering of centromeres and telomeres in fission yeast. J Cell Biol 121, 961–976.
Galli G, Hofstetter H, Birnstiel ML (1981). Two conserved sequence blocks within eukaryotic tRNA genes are major promoter elements. Nature 294, 626–631.
Gardner JM, Smoyer CJ, Stensrud ES, Alexander R, Gogol M, Wiegraebe W, Jaspersen SL (2011). Targeting of the SUN protein Mps3 to the inner nuclear membrane by the histone variant H2A.Z. J Cell Biol 193, 489–507.
Ghaemmaghami S, Huh WK, Bower K, Howson RW, Belle A, Dephoure N, O'Shea EK, Weissman JS (2003). Global analysis of protein expression in yeast. Nature 425, 737–741.
Gotta M, Laroche T, Formenton A, Maillet L, Scherthan H, Gasser SM (1996). The clustering of telomeres and colocalization with Rap1, Sir3, and Sir4 proteins in wild-type *Saccharomyces cerevisiae*. J Cell Biol 134, 1349–1363.
Gottschling DE, Aparicio OM, Billington BL, Zakian VA (1990). Position effect at *S. cerevisiae* telomeres: reversible repression of Pol II transcription. Cell 63, 751–762.
Guacci V, Hogan E, Koshland D (1997). Centromere position in budding yeast: evidence for anaphase A. Mol Biol Cell 8, 957–972.
Guldener U, Heck S, Fielder T, Beinhauer J, Hegemann JH (1996). A new efficient gene disruption cassette for repeated use in budding yeast. Nucleic Acids Res 24, 2519–2524.
Haeusler RA, Pratt-Hyatt M, Good PD, Gipson TA, Engelke DR (2008). Clustering of yeast tRNA genes is mediated by specific association of condensin with tRNA gene transcription complexes. Genes Dev 22, 2204–2214.
Harismendy O, Gendrel CG, Soularue P, Gidrol X, Sentenac A, Werner M, Lefebvre O (2003). Genome-wide location of yeast RNA polymerase III transcription machinery. EMBO J 22, 4738–4747.
Hartung M, Mirre C, Stahl A (1979). Nucleolar organizers in human oocytes at meiotic prophase I, studied by the silver-NOR method and electron microscopy. Hum Genet 52, 295–308.
Hayashi A, Ogawa H, Kohno K, Gasser SM, Hiraoka Y (1998). Meiotic behaviours of chromosomes and microtubules in budding yeast: relocalization of centromeres and telomeres during meiotic prophase. Genes Cells 3, 587–601.
Hediger F, Neumann FR, Van Houwe G, Dubrana K, Gasser SM (2002). Live imaging of telomeres: yKu and Sir proteins define redundant telomere-anchoring pathways in yeast. Curr Biol 12, 2076–2089.
Heun P, Laroche T, Raghuraman MK, Gasser SM (2001). The positioning and dynamics of origins of replication in the budding yeast nucleus. J Cell Biol 152, 385–400.
Hiraga S, Botsios S, Donaldson AD (2008). Histone H3 lysine 56 acetylation by Rtt109 is crucial for chromosome positioning. J Cell Biol 183, 641–651.
Hiraga S, Robertson ED, Donaldson AD (2006). The Ctf18 RFC-like complex positions yeast telomeres but does not specify their replication time. EMBO J 25, 1505–1514.
Iwase M, Luo J, Nagaraj S, Longtine M, Kim HB, Haarer BK, Caruso C, Tong Z, Pringle JR, Bi E (2006). Role of a Cdc42p effector pathway in recruitment of the yeast septins to the presumptive bud site. Mol Biol Cell 17, 1110–1125.
Jambunathan N, Martinez AW, Robert EC, Agochukwu NB, Ibos ME, Dugas SL, Donze D (2005). Multiple bromodomain genes are involved in restricting the spread of heterochromatic silencing at the *Saccharomyces cerevisiae* HMR-tRNA boundary. Genetics 171, 913–922.
Jin Q, Trelles-Sticken E, Scherthan H, Loidl J (1998). Yeast nuclei display prominent centromere clustering that is reduced in nondividing cells and in meiotic prophase. J Cell Biol 141, 21–29.
Kalmarova M, Smirnov E, Masata M, Koberna K, Ligasova A, Popov A, Raska I (2007). Positioning of NORs and NOR-bearing chromosomes in relation to nucleoli. J Struct Biol 160, 49–56.
Kassavetis GA, Bardeleben C, Kumar A, Ramirez E, Geiduschek EP (1997). Domains of the Brf component of RNA polymerase III transcription factor IIIB (TFIIIB): functions in assembly of TFIIIB-DNA complexes and recruitment of RNA polymerase to the promoter. Mol Cell Biol 17, 5299–5306.
Kassavetis GA, Braun BR, Nguyen LH, Geiduschek EP (1990). *S. cerevisiae* TFIIIB is the transcription initiation factor proper of RNA polymerase III, while TFIIIA and TFIIIC are assembly factors. Cell 60, 235–245.
Katou Y, Kanoh Y, Bando M, Noguchi H, Tanaka H, Ashikari T, Sugimoto K, Shirahige K (2003). S-phase checkpoint proteins Tof1 and Mrc1 form a stable replication-pausing complex. Nature 424, 1078–1083.
Kendall A, Hull MW, Bertrand E, Good PD, Singer RH, Engelke DR (2000). A CBF5 mutation that disrupts nucleolar localization of early tRNA biosynthesis in yeast also suppresses tRNA gene-mediated transcriptional silencing. Proc Natl Acad Sci USA 97, 13108–13113.
Kim SH, McQueen PG, Lichtman MK, Shevach EM, Parada LA, Misteli T (2004). Spatial genome organization during T-cell differentiation. Cytogenet Genome Res 105, 292–301.
Klein F, Laroche T, Cardenas ME, Hofmann JF, Schweizer D, Gasser SM (1992). Localization of RAP1 and topoisomerase II in nuclei and meiotic chromosomes of yeast. J Cell Biol 117, 935–948.
Kleinschmidt RA, LeBlanc KE, Donze D (2011). Autoregulation of an RNA polymerase II promoter by the RNA polymerase III transcription factor III C (TF(III)C) complex. Proc Natl Acad Sci USA 108, 8385–8389.
Maillet L, Gaden F, Brevet V, Fourel G, Martin SG, Dubrana K, Gasser SM, Gilson E (2001). Ku-deficient yeast strains exhibit alternative states of silencing competence. EMBO Rep 2, 203–210.
Marzouki N, Camier S, Ruet A, Moenne A, Sentenac A (1986). Selective proteolysis defines two DNA binding domains in yeast transcription factor tau. Nature 323, 176–178.
Michaelis C, Ciosk R, Nasmyth K (1997). Cohesins: chromosomal proteins that prevent premature separation of sister chromatids. Cell 91, 35–45.
Moqtaderi Z, Struhl K (2004). Genome-wide occupancy profile of the RNA polymerase III machinery in *Saccharomyces cerevisiae* reveals loci with incomplete transcription complexes. Mol Cell Biol 24, 4118–4127.
Moqtaderi Z, Wang J, Raha D, White RJ, Snyder M, Weng Z, Struhl K (2010). Genomic binding profiles of functionally distinct RNA polymerase III transcription complexes in human cells. Nat Struct Mol Biol 17, 635–640.
Newman AJ, Ogden RC, Abelson J (1983). tRNA gene transcription in yeast: effects of specified base substitutions in the intragenic promoter. Cell 35, 117–125.
Nishimura K, Fukagawa T, Takisawa H, Kakimoto T, Kanemaki M (2009). An auxin-based degron system for the rapid depletion of proteins in nonplant cells. Nat Methods 6, 917–922.

Noma K, Cam HP, Maraia RJ, Grewal SI (2006). A role for TFIIIC transcription factor complex in genome organization. Cell 125, 859–872.
Oza P, Jaspersen SL, Miele A, Dekker J, Peterson CL (2009). Mechanisms that regulate localization of a DNA double-strand break to the nuclear periphery. Genes Dev 23, 912–927.
Parada LA, McQueen PG, Misteli T (2004). Tissue-specific spatial organization of genomes. Genome Biol 5, R44.
Parelho V *et al*. (2008). Cohesins functionally associate with CTCF on mammalian chromosome arms. Cell 132, 422–433.
Roberts DN, Stewart AJ, Huff JT, Cairns BR (2003). The RNA polymerase III transcriptome revealed by genome-wide localization and activity-occupancy relationships. Proc Natl Acad Sci USA 100, 14695–14700.
Robinett CC, Straight A, Li G, Willhelm C, Sudlow G, Murray A, Belmont AS (1996). In vivo localization of DNA sequences and visualization of large-scale chromatin organization using lac operator/repressor recognition. J Cell Biol 135, 1685–1700.
Ruben GJ, Kirkland JG, MacDonough T, Chen M, Dubey RN, Gartenberg MR, Kamakaka RT (2011). Nucleoporin mediated nuclear positioning and silencing of HMR. PLoS One 6, e21923.
Rusche LN, Kirchmaier AL, Rine J (2002). Ordered nucleation and spreading of silenced chromatin in *Saccharomyces cerevisiae*. Mol Biol Cell 13, 2207–2222.
Schimmang T, Tollervey D, Kern H, Frank R, Hurt EC (1989). A yeast nucleolar protein related to mammalian fibrillarin is associated with small nucleolar RNA and is essential for viability. EMBO J 8, 4015–4024.
Schmid M, Arib G, Laemmli C, Nishikawa J, Durussel T, Laemmli UK (2006). Nup-PI: the nucleopore-promoter interaction of genes in yeast. Mol Cell 21, 379–391.
Schober H, Ferreira H, Kalck V, Gehlen LR, Gasser SM (2009). Yeast telomerase and the SUN domain protein Mps3 anchor telomeres and repress subtelomeric recombination. Genes Dev 23, 928–938.
Sexton T, Schober H, Fraser P, Gasser SM (2007). Gene regulation through nuclear organization. Nat Struct Mol Biol 14, 1049–1055.
Shu X, Shaner NC, Yarbrough CA, Tsien RY, Remington SJ (2006). Novel chromophores and buried charges control color in mFruits. Biochemistry 45, 9639–9647.
Simms TA, Dugas SL, Gremillion JC, Ibos ME, Dandurand MN, Toliver TT, Edwards DJ, Donze D (2008). TFIIIC binding sites function as both heterochromatin barriers and chromatin insulators in *Saccharomyces cerevisiae*. Eukaryot Cell 7, 2078–2086.
Sun FL, Elgin SC (1999). Putting boundaries on silence. Cell 99, 459–462.
Taddei A, Gasser SM (2004). Multiple pathways for telomere tethering: functional implications of subnuclear position for heterochromatin formation. Biochim Biophys Acta 1677, 120–128.
Taddei A, Hediger F, Neumann FR, Bauer C, Gasser SM (2004). Separation of silencing from perinuclear anchoring functions in yeast Ku80, Sir4 and Esc1 proteins. EMBO J 23, 1301–1312.
Tanabe H, Habermann FA, Solovei I, Cremer M, Cremer T (2002). Non-random radial arrangements of interphase chromosome territories: evolutionary considerations and functional implications. Mutat Res 504, 37–45.
Thompson M, Haeusler RA, Good PD, Engelke DR (2003). Nucleolar clustering of dispersed tRNA genes. Science 302, 1399–1401.
Towbin BD, Meister P, Gasser SM (2009). The nuclear envelope—a scaffold for silencing? Curr Opin Genet Dev 19, 180–186.
Valenzuela L, Dhillon N, Kamakaka RT (2009). Transcription independent insulation at TFIIIC-dependent insulators. Genetics 183, 131–148.
Venters BJ *et al*. (2011). A comprehensive genomic binding map of gene and chromatin regulatory proteins in *Saccharomyces*. Mol Cell 41, 480–492.
Wallace JA, Felsenfeld G (2007). We gather together: insulators and genome organization. Curr Opin Genet Dev 17, 400–407.
West AG, Gaszner M, Felsenfeld G (2002). Insulators: many functions, many mechanisms. Genes Dev 16, 271–288.